RF ACCELERATING SYSTEM FOR TARN II

K. Sato, A. Itano*, M. Fujita, M. Kodaira**, E. Tojyo, N. Yamazaki, A. Mizobuchi,
M. Kanazawa***, T. Kurihara, M. Takanaka****, S. Watanabe and M. Yoshizawa
Institute for Nuclear Study, University of Tokyo
Midori-cho, Tanashi-shi, Tokyo 188, Japan

Abstract

An rf accelerating cavity having a very wide range of tunable frequency from 0.61 MHz to 8.00 MHz has successfully been constructed. It is shown by low-level rf measurements of the cavity that no parasitic resonance distorts an rf accelerating voltage in this frequency range. Parasitic resonances observed at frequencies below 30 MHz are expected to give no serious disturbance on operation of the cavity. An equivalent lumped circuit model is proposed to explain origins of most of the resonances and rf behavior of the cavity.

Introduction

At the Institute for Nuclear Study, University of Tokyo, a heavy-ion synchrotron-cooler, TARN II, is under construction[1]. It is planned to accumulate and accelerate ions from the existing SF cyclotron and a heavy-ion linac. An rf accelerating system for TARN II is being developed to respond various demands such as synchronous capture of beams from the SF cyclotron and adiabatic capture of beams from the two injectors.

A previous paper[2] has presented design features of the cavity and rf acceleration parameters based on low-level rf measurements of a ferrite material. We have expected a frequency range of a factor of 11 in that paper. However, it is experimentally confirmed that the actual rf cavity can operate in a wider frequency range of a factor of 13.2; so that the rf acceleration parameters are improved appreciably as listed in Table 1.

Table 1 Rf acceleration parameters

Injection energy	> 2.92 MeV/u
Acceleration energy	< 1.3 GeV/u
Momentum spread at injection	< ±0.4%
Revolution frequency	0.305 - 3.51 MHz
Harmonic number	
Adiabatic capture/Acceleration	2
Synchronous capture	17
Acceleration frequency	0.61 - 8.00 MHz
Adiabatic capture/Acceleration	0.61 - 7.02 MHz
Synchronous capture	7.32 - 8.00 MHz
Maximum rf accelerating voltage	6 kV

Rf accelerating cavity

The rf cavity has a single-gap structure which consists of two ferrite-loaded quarter-wave coaxial resonators. A word "resonator" in this paper is used to express a half cavity. In order to produce an accelerating voltage at the gap, a push-pull mode excitation of the two resonators is achieved by the help of a "figure of eight" configuration of ferrite-bias windings. Cross section of the cavity has been shown in the previous paper.

Ferrite

Choice of a ferrite material with high incremental permeability at remanent state is vitally important to realize an rf cavity with a very wide frequency range. We have chosen a ferrite material, TDK SY-6.

Ferrite rings were once sintered at a high temperature, but those have again been heated at a higher temperature by the manufacturer to raise remanent permeability. Values of the permeability of 48 rings distribute from 969 to 1214 and the average is 1093. These 48 rings are alternately stacked in the two resonators according of the order of the increasing permeability to balance the two resonators electrically.

Measurements of the cavity with SY-6 show that a tunable frequency changes by a factor of 15.5 from 0.59 MHz to 9.18 MHz when a bias field changes from 0 AT/m to 2.59 kAT/m.

Electrical configuration

Difficulties in realizing an rf cavity with a very wide frequency range are summarized as follows.

1. Incremental permeability of a ferrite material with high remanent permeability largely varies at a low bias field region where a power supply for a bias current has no good stability.
2. Parasitic resonances probably occur within a required frequency range and within a frequency range below third harmonics of the required range, because the cavity consists of many ferrite rings, many copper cooling plates, many capacitors, the bias windings, etc. in a complicated configuration.
3. A capacitive divider type of rf voltage monitor possibly affects resonant frequencies of the parasitic resonances because the monitor neccessarily consists of large capacitances.
4. It is difficult to equip an anode rf choke for a final rf power amplifier outside the cavity without problems of parasitic resonances on it.
5. Rf leakages from dc input terminals of the bias windings and the anode choke should be kept as low as possible.

The TARN II rf cavity has been designed to overcome the above subjects as presented in the previous paper where seven design features have been listed. Success of the present cavity is largely due to these preparations because those allow adequate alteration on an electrical configuration of the cavity. The electrical configuration has been fixed as shown in Fig. 1.

Ultra-high vacuum

When beam pipes are heated at 350°C for baking, no heating problem is experienced in both inner surfaces of copper bus bars for the bias windings and of the ferrite rings without heat protection between the pipes and the ferrite rings. Ultra-high vacuum of the beam pipes has been achieved at a pressure of 1×10^{-10} Torr.

Present addresses: * National Institute of Radiological Sciences, Chiba-ken
** Toshiba Ltd., Keihin Works, Kanagawa-ken
*** Laboratoire National Saturne, CEN-Saclay, France
**** Mitsubishi Electric Corp., Nuclear Fusion Develop. Depart., Tokyo

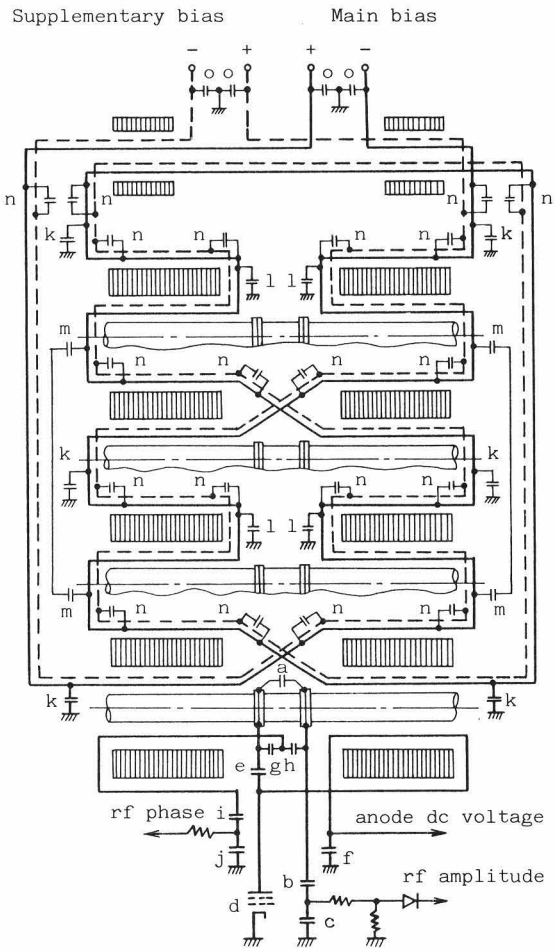

Fig. 1 Electrical configuration of the rf cavity. Capacitance values: a=100pF, b=25pF, c=1nF, d=25pF, e=140nF, f=117nF, g=125pF, h=125pF, i=200pF, j=40nF, k=100nF, l=200nF, m=100nF, n=200nF, and o=100nF.

Equivalent lumped circuits

An equivalent lumped circuit model of the TARN II rf cavity is proposed to explain origins of parasitic resonances. In all the circuits, windings such as bias windings, an anode choke, and an rf phase monitor are assumed to have proper self-inductances. In addition, mutual coupling between the resonators and the windings is assumed to be perfectly close.

Basic configuration of the rf cavity

Two resonators are connected to each other by the "figure of eight" configuration of the bias windings. An example of the windings with two turns is shown in Fig. 2. It should be noted in the figure that the two windings are separated from each other.

Two resonances appear. They are denoted by RES1 and RES2, and their resonant frequencies are denoted by f1 and f2, respectively: similar notations are used for other resonances in this paper.

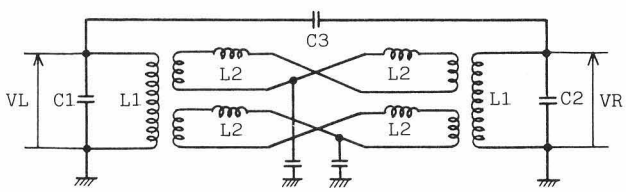

Fig. 2 Equivalent lumped circuit of an rf cavity with two bias windings.

In the fundamental resonance RES1, two rf voltages at left and right resonators, VL and VR, are excited in the opposite phase, that is, VL=-VR. The frequency f1 approximately is

$$f_1 = \frac{1}{2\pi}\sqrt{\frac{2}{L_1(C_1+C_2+4C_3)}} \quad . \tag{1}$$

In this resonance, no rf current flows on the bias windings; so that rf loss due to the bias windings is small.

In the parasitic resonance RES2, the two voltages are excited in the same phase, that is, VL=VR. The frequency f2 approximately is

$$f_2 = \frac{1}{2\pi}\sqrt{\frac{N(C_1+C_2+4C_3)}{2L_2(C_1C_2+C_1C_3+C_2C_3)}} \quad , \tag{2}$$

where N is a turn number of the bias windings. In this resonance, no rf voltage appears at cross-overs of the bias windings; so that pararell connection of all the proper self-inductances L2 influences f2.

It is known from Eqs. (1) and (2) that a large value of C3 and a small value of L2/N are effective to raise f2 when a summation C1+C2+4C3 is fixed at a given value to achieve the required frequency range. Therefore, the TARN II rf cavity has been designed by the use of small values of C1 and C2 as possible, and by the use of wide bus bars for the bias windings as possible, too.

It should be noted that the configuration of the bias windings shown in Fig. 2 can be modified to one shown in Fig. 3 equivalently in both rf performance and bias current. This new configuration is called a symmetric "figure of eight" one[3]. This is very helpful for providing a wide space around the accelerating gap of the cavity, because the cross-overs of the bias windings are reduced to half. The TARN II rf cavity is then based on this configuration as shown in Fig. 1; the wide space allows to equip capacitors for the anode choke inside the cavity, a winding type of rf phase monitor, and the capacitance C3 at the gap.

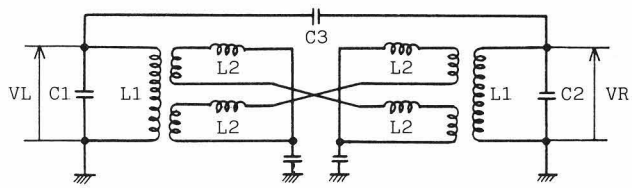

Fig. 3 Equivalent lumped circuit of an rf cavity with a symmetric "figure of eight" configuration of bias windings.

Rf phase monitor

The rf cavity is equipped with amplitude and phase monitors for an rf accelerating voltage. An equivalent lumped circuit of the monitors is shown in Fig. 4.

The rf amplitude monitor is of a simple capacitive divider type. A capacitance C8 works like C2 of Fig. 2; so that it lowers f2. However, because a small value of C8 is enough for the monitor, a frequency change is small.

A new type of rf phase monitor is equipped to avoid a decrease of f2. It is of a winding type as shown in Fig. 4.

An rf voltage VM at a top of C6 is expressed by the two voltages, VL and VR, when C6 ≪ C7, that is,

$$VM = -\frac{C_5}{C_4+C_5+C_6-\omega^2 C_6(C_4+C_5)}(VL-VR). \tag{3}$$

In the fundamental resonance RES1, the voltage VM can detect a correct rf phase because of VL=-VR. In the parasitic resonance RES2, the voltage VM vanishes because of VL=VR. Therefore, this type of monitor gives

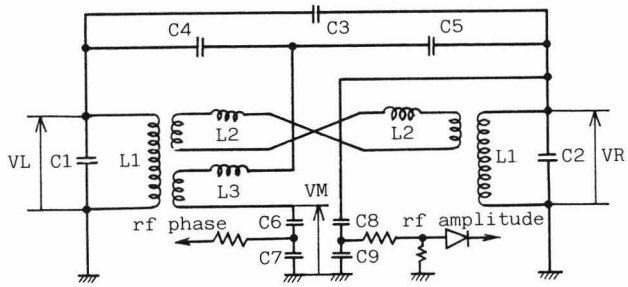

Fig. 4 Equivalent lumped circuit of rf voltage monitors.

no disturbance on f2 even when large values of C4, C5, and C6 are used.

It is known from Eq. (3) that a parasitic resonance RES3 appears. A frequency f3 is

$$f_3 = \frac{1}{2\pi}\sqrt{\frac{1}{L_3}\left(\frac{1}{C_4+C_5}+\frac{1}{C_6}\right)} \quad . \tag{4}$$

The frequency f3 is relatively low, because relatively large values of C4, C5, and C6 are used; those values should be adjusted to locate RES3 at a frequency above the required frequency range.

Anode rf choke

An anode rf choke for a final rf power amplifier is equipped inside the cavity. It is of a winding type as shown in Fig. 5. One end of the winding is connected to a resonator through capacitance for dc blocking and the other end is terminated by capacitance for rf grounding. A configuration of the winding is similar to the "figure of eight" one of the bias windings. This configuration is expected to raise the frequency f2 because the number N in Eq. (2) increases effectively.

An rf voltage VB at a dc input terminal of an rf grounding capacitance C11 is expressed by the two rf voltages, VL and VR, and an rf current I fed by an rf power source when capacitance of an rf power tube is ignored, that is,

$$VB = \frac{C_{10}}{C_{10}+C_{11}-\omega^2 L_4 C_{10} C_{11}}\left(VL+VR+\frac{1}{j\omega C_{10}}I\right) \quad . \tag{5}$$

In the fundamental resonance RES1, the voltage VB becomes small because of VL=-VR; so that this type of anode choke works well.

It is known from Eq. (5) that a parasitic resonance RES4 appears. A frequency f4 is

$$f_4 = \frac{1}{2\pi}\sqrt{\frac{1}{L_4}\left(\frac{1}{C_{10}}+\frac{1}{C_{11}}\right)} \quad . \tag{6}$$

The frequency f4 is low, because large values of C10 and C11 are neccesary for a good performance of the anode choke; those values should be adjusted to locate RES4 at a frequency below the required frequency range. At high frequencies in comparison with f4, this type of anode choke is expected to work well even in the case of VL=VR, because the denominator of Eq. (6) becomes very large.

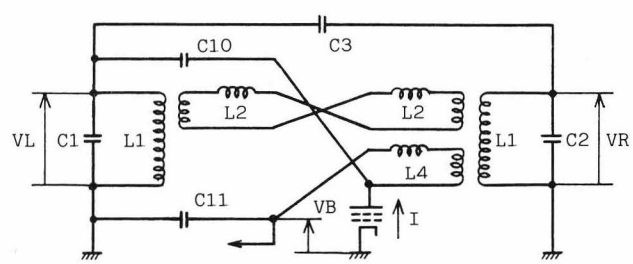

Fig. 5 Equivalent lumped circuit of an anode rf choke.

Low-level rf measurements

Basic rf characteristics of the TARN II rf cavity

Frequency of the fundamental resonance, shunt impedance, and Q-factor are measured as a function of bias current by a vector impedance meter. The results are shown in Fig. 6 as a function of the frequency.

A tunable frequency of the cavity itself ranges from 0.59 MHz to 9.18 MHz. However, a usable frequency is limited from 0.61 MHz to 8 MHz due to parasitic resonances on the anode choke. The lowest value of the shunt impedance is obtained at 250 Ω around 5 MHz.

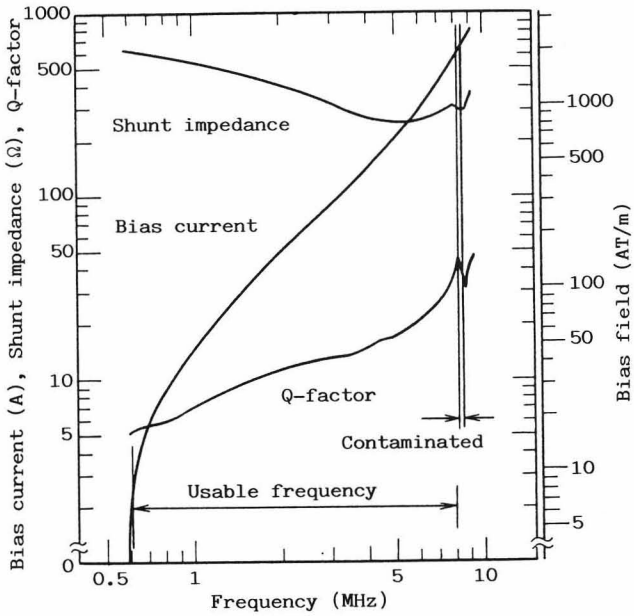

Fig. 6 Tunable frequency, shunt impedance, Q-factor, and bias current(bias field).

Resonances

An rf signal from a signal generator in frequency-sweep mode is once terminated by 50 Ω and is then fed to the cavity through a series resistance of 1.5 kΩ. Rf voltages at appropriate points of the cavity are then observed by an oscilloscope.

Two voltages at the left and right resonators, VL and VR, together with a summation VL-VR or a subtraction VL+VR are shown in Figs. 7(a) and 7(b).

The resonance in Fig. 7(a) is identified to the fundamental one RES1; the relation of VL=-VR is valid.

The resonance observed at a high frequency of 29.0 MHz in Fig. 7(b) is identified to the parasitic one RES2; the relation of VL=VR is approximately valid.

The resonance observed at a middle frequency of 16.1 MHz in Fig. 7(b) is identified to the parasitic one RES3. This resonance is clearly observed at the left resonator but is not observed at the right one.

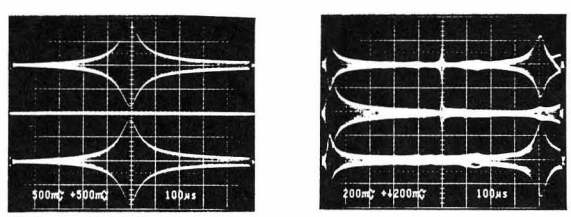

(a) 0.1 - 3 MHz (b) 1 - 30 MHz

Fig. 7 Rf voltages at the left and right resonators at a bias current of 30 A.
(a) and (b) upper: left VL, lower: right VR
(a) middle: VL+VR, (b) middle: VL-VR

Therefore, the capacitive divider type of rf amplitude moinitor is equipped at the right resonator to avoid harmonic contamination due to RES3.

This identification of RES3 is also supported by the observation shown in Figs. 8(a) and 8(b), which show an rf voltage VM at a top of the rf phase monitor.

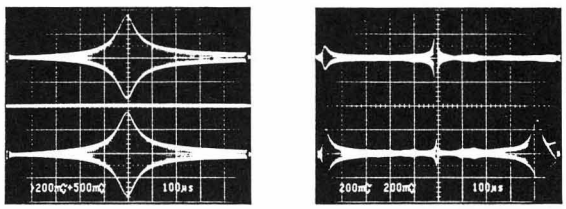

(a) 0.1 - 3 MHz (b) 1 - 30 MHz

Fig. 8 Rf voltage at the rf phase monitor at a bias current of 30 A.
(a) and (b) upper: rf phase monitor VM
lower: left resonator VL
(a) middle: VM+VL in appropriate amplitude

It is known from the figures that the rf phase monitor correctly detects a phase of the rf voltage and the monitor is insensitive to the resonance RES2.

Rf voltages at dc input terminals of the anode choke and the bias windings at no bias current are shown in Figs. 9(a) and 9(b).

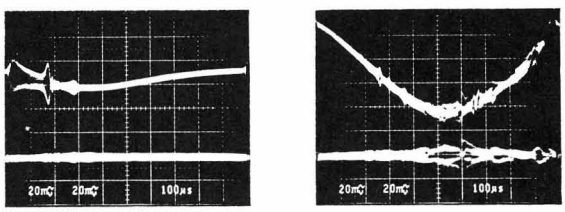

(a) 0.1 - 3 MHz (b) 1 - 30 MHz

Fig. 9 Rf voltages at dc input terminals of anode rf choke and bias windings at no bias current.
(a) and (b) upper: anode rf choke
lower: ferrite-bias windings

Parasitic resonances are observed at a frequency of 0.58 MHz and at a frequency of 8.30 MHz at the dc input terminal of the anode choke. The former is identified to the resonance RES4. A usable frequency of the cavity is then limited to the range of 0.61-8 MHz to avoid an rf leakage through the anode choke.

The parasitic resonance RES2 is not observed at the dc input terminal of the anode choke as expected.

A parasitic resonance is observed at the both terminals at a frequency of 0.95 MHz within the usable frequency range. However, its amplitude is kept small even when the fundamental resonance pass over it.

Quantitative prediction of resonant frequencies

Values of the proper self-inductances L2, L3 and L4 are based on straight bus bars with an uniform rectangular cross-section and a given length. Values of the capacitances C1, C2, and C3 for prediction of f1 and f2 include not only themselves shown in Fig. 1 but also capacitances of such as the accelerating gap and the rf voltage monitors, effectively. The number N in Eq. (2) should include an effect of the "figure of eight" configuration of the anode choke.

Table 2 shows a comparison between the observation and the prediction at no bias current. Close agreement in f3 and f4 is obtained; this implies a nice estimation of L3 and L4, therefore, L2 as well. However, discrepancy in f1 and f2 is relatively large. This is probably due to an effect of missing capacitances which may exist between the bias windings and the resonators.

Table 2 Resonant frequencies at no bias current

Resonances	RES1	RES2	RES3	RES4
Observation	0.59MHz	29.1MHz	16.1MHz	0.58MHz
Prediction	0.97MHz	62.4MHz	12.8MHz	0.53MHz
Inductance	L1=59μH	L2=1.3μH	L3=1.4μH	L4=1.4μH
Capacitance	C1=25pF		C4=125pF	C10=140nF
	C2=25pF		C5=125pF	C11=117nF
	C3*=215pF	C3*=188pF	C6=200pF	

* Effective values

Bias response

A power supply for the main bias current is controlled to produce a square-wave current; a response of rf amplitude of the fundamental resonance is observed under the condition of the resonance in and out. The amplitude observation is made by a subtraction of two rf voltages at the left and right resonators, because this cancels voltages induced by the current change.

The bias response at a low bias current is shown in Figs. 10(a) and 10(b). It is noticed from Fig. 10(b) that the amplitude response is faster than the current response; so that a bias response of the ferrite itself is considered to be faster than 0.8 ms reduced from the figure. At a high bias current, the ferrite bias response is considered to be faster than 0.3 ms.

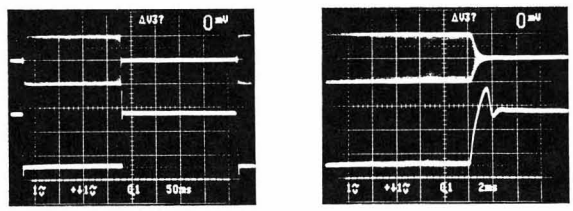

(a) overall view (b) magnified view

Fig. 10 Bias response of rf amplitude and main bias current at top of 90 A and bottom of 18 A.
(a) and (b) upper: rf amplitude
lower: main bias current

Discussion

The TARN II rf cavity is tunable in the frequency range of 0.59-9.2 MHz. However, the parasitic resonance RES4 and the one at 8.3 MHz restrict this range to 0.61 -8 MHz. Because the both parasitic frequencies change at the same time when a value of the capacitance for rf grounding of the anode choke is altered, it is difficult to compromise them separately. Our experience show that the latter and the one at 0.95 MHz are due to own resonances of capacitors for rf grounding of the anode choke and the bias windings. When a range wider than the present range is required, such capacitors should be replaced by ones with better rf characteristics.

The resonance RES3 at 16.1 MHz observed at the rf phase monitor will not affect an rf phase detection, because a heterodyne technique will be applied to attain the fundamental component of rf signals.

The proper self-inductances of the windings play an important role in the rf behavior of the cavity and the resonances. A study of origin of the missing capacitance is neccessary for a full understanding of rf characteristics of the cavity.

References

1. T. Katayama, "Heavy Ion Accelerator and Cooler - TARN II", in these proceedings.
2. K. Sato et al., "Rf System for "TARN II"", IEEE Trans. on Nucl. Sci., NS-32 (1985) 2828-2831.
3. K. Kaspar and M. Emmerling, "New Configuration of the Bias Windings in the SIS Prototype Cavity", GSI Scientific Report 1983, 1984, p.324.